

1-1-2011

Four-parameter model for polarization-resolved rough-surface BRDF

Ingmar G. E. Renhorn

Tomas Hallberg

David Bergström

Glenn D. Boreman

University of Central Florida

Find similar works at: <https://stars.library.ucf.edu/facultybib2010>

University of Central Florida Libraries <http://library.ucf.edu>

This Article is brought to you for free and open access by the Faculty Bibliography at STARS. It has been accepted for inclusion in Faculty Bibliography 2010s by an authorized administrator of STARS. For more information, please contact STARS@ucf.edu.

Recommended Citation

Renhorn, Ingmar G. E.; Hallberg, Tomas; Bergström, David; and Boreman, Glenn D., "Four-parameter model for polarization-resolved rough-surface BRDF" (2011). *Faculty Bibliography 2010s*. 1813.

<https://stars.library.ucf.edu/facultybib2010/1813>

Four-parameter model for polarization-resolved rough-surface BRDF

Ingmar G. E. Renhorn,^{1,*} Tomas Hallberg,¹ David Bergström,¹
and Glenn D. Boreman²

¹FOI – Swedish Defense Research Agency, P.O. Box 1165, SE-581 11, Linköping, Sweden
²University of Central Florida, CREOL/College of Optics & Photonics, Orlando, FL 32816-2700, USA
* ingmar.renhorn@foi.se

Abstract: A modeling procedure is demonstrated, which allows representation of polarization-resolved BRDF data using only four parameters: the real and imaginary parts of an effective refractive index with an added parameter taking grazing incidence absorption into account and an angular-scattering parameter determined from the BRDF measurement of a chosen angle of incidence, preferably close to normal incidence. These parameters allow accurate predictions of *s*- and *p*-polarized BRDF for a painted rough surface, over three decades of variation in BRDF magnitude. To characterize any particular surface of interest, the measurements required to determine these four parameters are the directional hemispherical reflectance (DHR) for *s*- and *p*-polarized input radiation and the BRDF at a selected angle of incidence. The DHR data describes the angular and polarization dependence, as well as providing the overall normalization constraint. The resulting model conserves energy and fulfills the reciprocity criteria.

©2011 Optical Society of America

OCIS codes: (290.1483) BRDF; (290.5820) Scattering measurements; (290.5880) Rough surfaces.

References and links

1. K. E. Torrance, and E. M. Sparrow, "Theory for off-specular reflection from roughened surfaces," *J. Opt. Soc. Am.* **57**(9), 1105–1114 (1967).
2. J. R. Maxwell, J. Beard, S. Weiner, D. Ladd, and S. Ladd, "Bidirectional reflectance model validation and utilization," Technical Report AFAL-TR-73–303, Environmental Research Institute of Michigan (ERIM), October 1973.
3. J. C. Jafolla, D. J. Thomas, J. W. Hilgers, W. R. Reynolds, and C. Blasband, "Theory and measurement of bidirectional reflectance for signature analysis," *Proc. SPIE* **3699**, 2–15 (1999).
4. P. Beckmann and A. Spizzichino, "The Scattering of Electromagnetic Waves from Rough Surfaces," (Pergamon Press, 1963).
5. X. D. He, K. E. Torrance, F. X. Sillion, and D. P. Greenberg, "A comprehensive physical model for light reflection," *Comput. Graph.* **25**(4), 175–186 (1991).
6. D. B. Goldman, B. Curless, A. Hertzmann, and S. M. Seitz, "Shape and spatially-varying BRDFs from photometric stereo," *IEEE Trans. Pattern Anal. Mach. Intell.* **32**(6), 1060–1071 (2010).
7. R. Priest, and T. Germer, "Polarimetric BRDF in the microfacet model: theory and measurements," *Proc. Military Sensing Symposia Specialty Group on Passive Sensors*, Vol. 1, pp. 169–181 (Infrared Information Analysis Center, Ann Arbor, MI, August 2000), available at <http://physics.nist.gov/Divisions/Div844/publications/germer/GermerPriestMicroFacet.pdf>
8. T. A. Germer, and E. Marx, "Ray model of light scattering by flake pigments or rough surfaces with smooth transparent coatings," *Appl. Opt.* **43**(6), 1266–1274 (2004).
9. I. G. Renhorn, and G. D. Boreman, "Analytical fitting model for rough-surface BRDF," *Opt. Express* **16**(17), 12892–12898 (2008).
10. J. Greffet, and M. Nieto-Vesperinas, "Field theory for generalized bidirectional reflectivity: derivation of Helmholtz's reciprocity principle and Kirchhoff's Law," *J. Opt. Soc. Am. A* **15**(10), 2735–2744 (1998).
11. J. Stover, *Optical Scattering, Measurement and Analysis* (SPIE Press, 1995).
12. B. G. Hoover, and V. L. Gamiz, "Coherence solution for bidirectional reflectance distributions of surfaces with wavelength-scale statistics," *J. Opt. Soc. Am. A* **23**(2), 314–328 (2006).
13. C. F. Bohren, and D. R. Huffman, *Absorption and Scattering of Light by Small Particles*, (Wiley-Interscience, New York, 1983).

14. R. G. Priest, and S. R. Meier, "Polarimetric microfacet scattering theory with applications to absorptive and reflective surfaces," *Opt. Eng.* **41**(5), 988–993 (2002).
 15. F. Nicodemus, J. Richmond, J. Hsia, I. Ginsburg, and T. Lamparis, "Geometrical considerations and nomenclature for reflectance," *Nat. Bur. Stand. (U.S.) Monograph* 160 (1977).
 16. D. A. Haner, B. T. McGuckin, R. T. Menzies, C. J. Bruegge, and V. Duval, "Directional-hemispherical reflectance for spectralon by integration of its bidirectional reflectance," *Appl. Opt.* **37**(18), 3996–3999 (1998).
 17. M. J. Persky, and M. Szczesniak, "Infrared, spectral, directional-hemispherical reflectance of fused silica, Teflon polytetrafluoroethylene polymer, chrome oxide ceramic particle surface, Pyromark 2500 paint, Krylon 1602 paint, and Duraflect coating," *Appl. Opt.* **47**(10), 1389–1396 (2008).
 18. H. Holl, "Specular reflection and characteristics of reflected light," *J. Opt. Soc. Am.* **57**(5), 683–690 (1967).
-

1. Introduction

Polarimetric imaging is of growing interest in the remote sensing community. The utility of the technique has mainly been in areas where flat surfaces of manmade materials are involved such as surfaces in the urban environment or anomaly detection of targets such as surface laid mines. Characterization of the state of the sea surface is another area of applicability. The predictive capability of polarimetric Bidirectional Reflectance Distribution Functions (pBRDF) are however limited and more work is needed on developing an understanding of various types of surfaces. In the scene simulation community where simplicity is at premium, empirical models based on fitting to observations and interpolating where data is missing has become very commonplace. In these cases the physical basis is not being considered.

One class of semi-empirical models is based on geometrical optics and statistical description of surface facet slope distributions. These types of models can be represented by the Torrance-Sparrow [1] model from 1967, and they require limitations on roughness relative to the wavelength and also generally require masking and shadowing functions. A further development of the semi-empirical model with respect to polarization and originally applied to painted surfaces was the Maxwell-Beard [2] model. Here, the Fresnel equation is invoked using half the angle between incident and reflected beam direction. Dielectric surfaces in this model are typically assumed to have a complex index of refraction $n \sim 1.65$ based on past measurements. Also this model requires masking and shadowing. The Sanford-Robertson model [3] is often used in signature prediction application. As in many other models, the diffuse and specular part of the BRDF is separated. Fresnel reflectance behavior is approximated in a simplified function.

Many physical models have their origin in Kirchhoff integral of scalar diffraction theory. This approach to rough surfaces has been treated thoroughly by Beckmann [4]. When applying physical modeling to BRDF, many of the semi-empirical approaches are used such as masking and shadowing [5]. Polarimetric BRDF is required in order to model reflected polarized radiance. Fresnel reflectance has been incorporated in e.g. micro-facet surface representation. A reason behind the development of a new model is some dissatisfaction with present models generally available in physics-based scene-simulation software. A criticism that is valid is also the limited performance with respect to predictive capability of the present low dimensionality models [6]. It is therefore motivated to further explore new approaches to pBRDF modeling.

There exist models for polarimetric BRDF in the literature, for instance [7,8]. However, these models are generally quite complex, and rather limited in applicability with respect to scattering angles and surface roughness. Due to these limitations, multiple functions with complementary sets of parameters are needed in the fitting of observed scattering to the model. In a previous article [9] we presented a physics-based analytical model for rough-surface pBRDF, which required 14 fitting parameters to predict *s*-polarized BRDF measurements. A somewhat different approach is taken here, which may be conceptually visualized as an outward-propagating random phasefront specified at a small distance above the surface itself. The property of this phasefront is related in a non-trivial way to the physical interaction of the radiation with the surface. Adopting a description in directional cosines, which is closely related to radiometry, a significant simplification of our model is obtained. The complete relationship of the scattered phasefront to the surface statistics is treated in detail in [10].

An important aspect of the present work is to find a strategy that can lead to realistic pBRDF using a limited set of data, primarily directional hemispherical data that are easy to measure. Ultimately, a method to obtain an approximate scattering parameter without making a detailed pBRDF measurement is desired. The model has been tested on a number of painted surfaces where a challenging example is given here. Future tests will show the generality in the present approach with respect to the physical phenomena in the material represented by the effective complex index of refraction and the effective roughness parameter.

2. Theory

Directional distribution of reflectance flux is defined by the BRDF. The BRDF is material and wavelength dependent resulting in a multitude of application dependent models.

Mathematically the BRDF is expressed as

$$f_{BRDF}(\theta_i, \varphi_i, \theta_r, \varphi_r, \lambda) = \frac{L(\theta_r, \varphi_r)}{E(\theta_i, \varphi_i)} \quad [sr^{-1}] \quad (1)$$

The resulting outcome of the BRDF depends on the material scattering properties and the surface spectral properties. Many models have been proposed ranging from physics based models to empirical models. The connection between physical optics and radiometry is well established [10] although there are still many issues to be studied. In the next step we will use a phase screen approximation that can lead to a coherence model of surface scattering. In this approximation, a virtual surface just above the actual surface is adopted. If the surface field is a scattered coherent field, the angular dependence of that scattered field is related to the BRDF and also related to the correlation function. For a quasi-homogeneous source, the radiance is proportional to the Fourier transform of the field correlation at the virtual surface.

The derivation of the BRDF from physical optics is non-trivial. Here, the function is based on a number of physically reasonable assumptions. The relevance of these assumptions is judged from the capability to generalize the BRDF for the specific material. Since the assumptions will vary with the surface properties, so will the BRDF. This means that also the functional form of the BRDF will vary with the surface properties. As an example, if the surface field covariance function follows an exponential behavior, the basic shape of the BRDF will be described by a Lorentz or Cauchy function. If the surface properties results in a Gaussian covariance function, the basic shape of the BRDF will be described by a Gaussian function. A more general BRDF describing also intermediate cases is the plasma dispersion function alternatively the Voigt function. Also a generalized Cauchy function is sometimes used for describing an autocovariance function that deviates from the Gaussian or Lorentzian shapes. Other shapes can of course also be invoked. For the painted surface presently under study, the following assumptions based on principles without proof are being made:

The basic shape of the BRDF can be described by a Lorentzian function.

The directional hemispherical reflectance (DHR) can be described by Fresnel equations using effective complex index of refraction.

The effective surface rms roughness scales with the angle of incidence and the scattering angle.

The effective surface roughness scales with the effective surface absorption.

A crucial difference is that our use of the Fresnel equation is different from what is generally accepted in the bistatic case. Stover [11] e.g. uses the geometric mean approximation, i.e. $\sqrt{F_s(\theta_i)F_s(\theta_r)}$. This approximation is here replaced by $F((\sin(\theta_i) + \sin(\theta_r))/2)$, now also being used for both s- and p-polarization. The introduction of this approximation has a profound influence on the applicability of the present model. The masking and shadowing function that is commonly introduced also in scalar models is no longer needed. The use of the mean of the angles instead of mean of directional cosines works less satisfactory in the experimental analysis.

The total reflectance of a surface is defined by the DHR and is the integral of the BRDF over all scattering angles

$$DHR^q(\alpha_i, \lambda) = \int_{-\sqrt{1-\alpha^2}^{-1}}^{\sqrt{1-\alpha^2}} \int_0^1 f_{pBRDF}^q(\alpha_i, \alpha, \beta, \lambda) d\alpha d\beta \quad (2)$$

where α and β are directional cosines and q stands for s- or p-polarization. Conservation of energy is secured by scaling the pBRDF with DHR results.

In the DHR measurements, input radiation is polarized while the detected radiation is the sum of all polarization states. This means that possible change of polarization is absorbed into the effective index of refraction. Provided depolarization and/or change of polarization are small, the model can be given simple polarimetric interpretations and constitutes a substantial improvement compared to presently commonly used models. The model can certainly be extended to other components in the Mueller matrix when needed. It is however of great benefit to have models that are relevant with respect to parameters actually being measured.

The geometry and the directional cosines are shown in Fig. 1. The angle of incidence is taken to be along the x/z-plane.

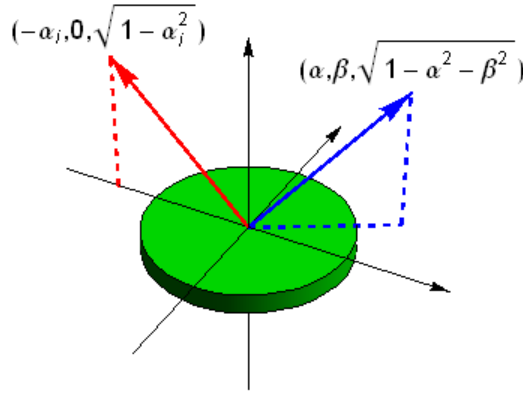


Fig. 1. Geometry of the pBRDF model. The red arrow shows the direction to the source and the blue arrow illustrates a scattering direction.

Assuming separability between the two orthogonal directions both with respect to geometry and polarization, the proposed pBRDF for a painted surface is as follows:

$$f_{pBRDF}^s = \frac{\sigma_N^s}{(\alpha - \alpha_i)^2 + \frac{1}{4}(\sqrt{1-\alpha_i^2} + \sqrt{1-\alpha^2})^2 \rho_{s,\alpha}^2} \frac{1}{\beta^2 + \frac{1}{4}(1 + \sqrt{1-\beta^2})^2 \rho_{p,\beta}^2} \times F_s((\alpha + \alpha_i)/2, n - ik) F_p(\beta/2, n - ik) \quad (3a)$$

$$f_{pBRDF}^p = \frac{\sigma_N^p}{(\alpha - \alpha_i)^2 + \frac{1}{4}(\sqrt{1-\alpha_i^2} + \sqrt{1-\alpha^2})^2 \rho_{p,\alpha}^2} \frac{1}{\beta^2 + \frac{1}{4}(1 + \sqrt{1-\beta^2})^2 \rho_{s,\beta}^2} \times F_p((\alpha + \alpha_i)/2, n - ik) F_s(\beta/2, n - ik) \quad (3b)$$

Since the parameter σ_N^s and σ_N^p are linear in the BRDF equations 3a and 3b, these normalization parameters can easily be determined from the relation

$$\sigma_N^0 F_q(\alpha_i, n-ik) = \int_{-\sqrt{1-\alpha^2}^{-1}}^{\sqrt{1-\alpha^2}} \int_0^1 f_{pBRDF}^q(\alpha_i, \alpha, \beta, \lambda) d\alpha d\beta. \quad (4)$$

The parameter σ_N^0 is introduced due to the observation that the directional hemispherical reflectance does not always approach one when the angle of incidence is approaching 90 degrees. F_q is the Fresnel reflection coefficient based on the effective complex index of refraction of the material.

ρ_q is given by

$$\rho_{q,\alpha} = \rho_0 \frac{(1 - F_q((\alpha + \alpha_i)/2, n-ik))}{(1 - F_q(0, n-ik))} \quad (5a)$$

$$\rho_{q,\beta} = \rho_0 \frac{(1 - F_q(\beta/2, n-ik))}{(1 - F_q(0, n-ik))} \quad (5b)$$

where ρ_0 is a constant that does not change with polarization. The angular scattering governed by the ρ_0 parameter is closely related to the surface height autocorrelation and slope distribution [12]. The modification of the roughness parameter ρ_q into an effective roughness parameter is based on the assumption that there is a relation between layer thickness being illuminated and participating in the scattering process and the angle dependent Fresnel reflectance of the material. This modification reminds one of the shadowing/masking invoked in the microfacet scattering. This modification is also qualitatively in accordance with experimental observations. A more elaborate modeling of the roughness parameter will probably give a better fit with observations, especially at large angles of incidence. Simplicity is however at a premium in the present model development.

Certain assumptions have to be made with respect to polarized illumination and polarimetric detection. For unpolarized illumination and non-polarizing detection, the BRDF function can be approximated by the mean of the polarimetric BRDF or

$$f_{BRDF} = \frac{f_{pBRDF}^s + f_{pBRDF}^p}{2}. \quad (6)$$

This is the most common use of BRDF functions in scene simulations. Since the BRDF function is often fitted to measurements using s-polarization, an error is introduced in the simulation. In polarimetric imaging, the polarimetric BRDF function is needed even if the illumination is unpolarized. The depolarization properties are not resolved in the present treatment. It is straightforward to add this to the model but often this information is lacking, which is why it is not presently invoked. Assuming single scattering, polarization properties close to the microfacet model can be expected. For future use, the polarimetric result for the geometry used here is given below, expressed in directional cosines. Using Stokes' formalism of representing polarization states, the relationship can be expressed as [13,14]

$$\vec{S}_r = \hat{R}(-\theta_r) \hat{f}_{pBRDF} \hat{R}(\theta_i) \vec{S}_i$$

where \vec{S}_q are the Stokes vectors and $\hat{R}(\theta)$ is the Mueller rotation matrix given by

$$\hat{R}(\theta) = \begin{pmatrix} 1 & 0 & 0 & 0 \\ 0 & \cos(2\theta) & \sin(2\theta) & 0 \\ 0 & -\sin(2\theta) & \cos(2\theta) & 0 \\ 0 & 0 & 0 & 1 \end{pmatrix} \quad (7)$$

and

$$\hat{f}_{pBRDF} = \frac{1}{2} \begin{pmatrix} f^s + f^p & f^s - f^p & 0 & 0 \\ f^s - f^p & f^s + f^p & 0 & 0 \\ 0 & 0 & 2\sqrt{f^s f^p} & 0 \\ 0 & 0 & 0 & 2\sqrt{f^s f^p} \end{pmatrix} \quad (8)$$

where circular polarization is ignored.

The Stokes vector component for s-polarized illumination, S^s , is given by

$$S^s = \begin{pmatrix} \frac{g f^s + \beta^2 f^p}{g + \beta^2} \\ \frac{(g f^s - \beta^2 f^p)(h - \alpha_i^2 \beta^2) + 4\sqrt{g h \alpha_i^2 f^s f^p} \beta^2}{(g + \beta^2)(h + \alpha_i^2 \beta^2)} \\ \frac{2(\sqrt{h \alpha_i^2 \beta^2} (g f^s - \beta^2 f^p) - \sqrt{g \beta^2 f^s f^p})(h - \alpha_i^2 \beta^2)}{(g + \beta^2)(h + \alpha_i^2 \beta^2)} \\ 0 \end{pmatrix} \quad (9)$$

and for p-polarized illumination, S^p , is given by

$$S^p = \begin{pmatrix} \frac{g f^p + \beta^2 f^s}{g + \beta^2} \\ \frac{(\beta^2 f^s - g f^p)(h - \alpha_i^2 \beta^2) - 4\sqrt{g h \alpha_i^2 f^s f^p} \beta^2}{(g + \beta^2)(h + \alpha_i^2 \beta^2)} \\ \frac{2(\sqrt{h \alpha_i^2 \beta^2} (\beta^2 f^s - g f^p) + \sqrt{g \beta^2 f^s f^p})(h - \alpha_i^2 \beta^2)}{(g + \beta^2)(h + \alpha_i^2 \beta^2)} \\ 0 \end{pmatrix} \quad (10)$$

where

$$g = \left(\alpha \sqrt{1 - \alpha_i^2} + \alpha_i \sqrt{1 - \alpha^2 - \beta^2} \right)^2 \quad (11)$$

and

$$h = \left((\alpha^2 + \beta^2) \sqrt{1 - \alpha_i^2} + \alpha \alpha_i \sqrt{1 - \alpha^2 - \beta^2} \right)^2. \quad (12)$$

A non-polarimetric sensor will detect the S_0 component of the Stokes vector. From this it is obvious that $S_0^s = f^s$ and $S_0^p = f^p$ for $\beta = 0$. For $\beta = 1$, $g = 0$ resulting in $S_0^s = f^p$ and $S_0^p = f^s$.

As discussed above, the full Mueller matrix is quite complex. By disregarding circular polarization, a simplified result is obtained for s- and p-polarized illumination. Using these results, the linear polarization can be obtained for all scattering angles.

3. Experimental results

We illustrate our approach using DHR and BRDF data for a painted rough surface, measured at 3.39 micrometer wavelength, over a range of angles of incidence from 0 to 80 degrees. BRDF measurements were made at 0.5 degree increments of scattering angle in the plane of incidence ($\beta = 0$), over a range from -80 to 80 degrees. The surface was chosen as an example for the fitting technique because it showed a significant amount of forward scatter for high angles of incidence, which is governed by the variation of reflectance as a function of both angles of incidence and scattering. This is representative of the challenge in modelling rough-surface BRDF and is why this particular surface data was chosen for illustration. Smoother surfaces can generally be handled more easily, and would also be amenable to description by our analytical model.

The DHR was first used in order to determine the overall reflectance as a function of angle of incidence of linearly polarized radiation. The DHR measurements [15–17] were made using a FTIR spectrometer and IR integrating sphere, with the beam incident on the sample at a range of incident angles from 10° to 80° , in both s and p polarizations. The DHR data quoted in this article were evaluated at $3.39 \mu\text{m}$, to match the wavelength at which the BRDF data were measured. In this type of measurement, the depolarization of the scattered radiation is not determined. The effective complex index of refraction obtained from the fitting of the observed measurements to Fresnel equations therefore will include also the depolarization part. The result will therefore strictly speaking be relevant only for non-polarimetric imaging. If depolarization is small, results will also be relevant for polarimetric imaging. In order to take depolarization into account in more detail, the model has to be further developed. This will also require more elaborate measurement techniques in order to determine the degree of depolarization.

We found the angular and polarization dependence of the DHR measurements to be quite similar in form to the corresponding behavior of the Fresnel coefficients at the planar boundary of a homogeneous lossy medium [18]. Thus, we were led to represent the scattering surface simply as an interface between air and a effective complex index of refraction $n-ik$, which yields a significant simplification in the model, while preserving the main features of the behavior. As seen in Fig. 2, the DHR data sets for both polarizations were fitted (including a small additive offset) to the Fresnel equations using a least-squares fit, which allowed determination of an effective value for $n-ik$. The good fit to the Fresnel equation can possibly be understood from the fact that the diffuse scattering dominates at small angles where the reflectance is changing only slowly while the scattering at large angles is more specular.

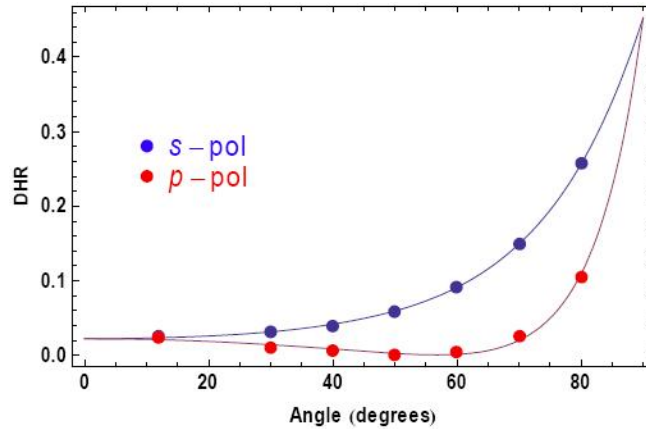


Fig. 2. Hemispherical (DHR) data for s- and p-polarizations at $3.39 \mu\text{m}$ as a function of angle of incidence for the green paint. The fitted values were $\sigma_N^0 = 0.4528$, $n = 1.526$ and $k = 0.193$.

The quite simple DHR measurement determines three of the four parameters needed in order to predict the pBRDF, namely the normalization of pBRDF and the effective complex index of refraction. The fourth parameter can be determined from any reasonable scattering experiment with specified polarization and angle of incidence.

The BRDF data was measured with a Surface Optics Corporation SOC-200 bidirectional reflectometer using a $3.39 \mu\text{m}$ laser. Although the instrument is computer controlled, the measurement process is time consuming. The DHR measurements are used in the normalization of the BRDF measurements.

When performing individual fittings for each specific angle of incidence, it was observed that the roughness parameter ρ_q was not constant as illustrated in Fig. 3. It was noticed that the angular behavior seen in Fig. 3 has an approximately complementary dependence to that seen in Fig. 2. This behavior was included in Eq. (5). This equation can certainly be refined by including further shielding at large angles not accounted for in the model. Deviations from predicted values are therefore expected at large angles.

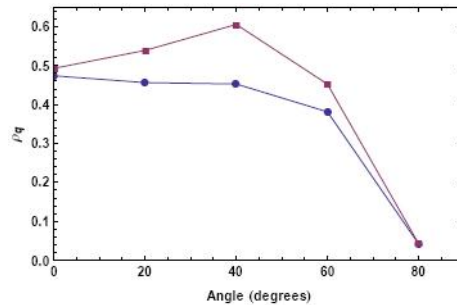


Fig. 3. Variations of the roughness parameter ρ_q for s- (blue curve) and p-polarizations (red curve).

In the following, the predictive power of the model will be shown based on two measurements of the roughness parameter including the modification given in Eq. (5). The first example is for normal angle of incidence and s-polarization, shown in Fig. 4a. The second one is for 20 degrees angle of incidence and s-polarization, shown in Fig. 4b.

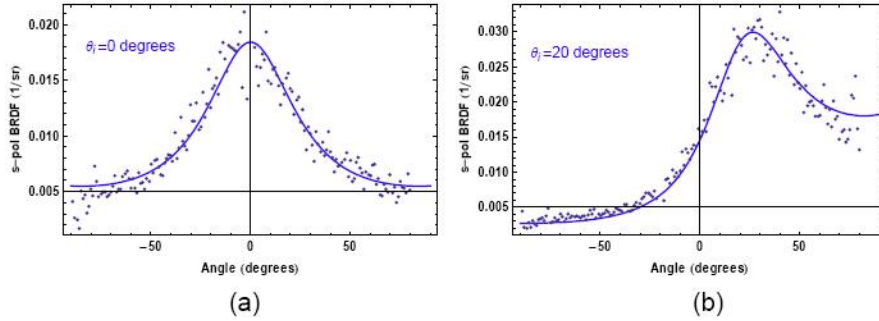


Fig. 4. The pBRDF model was fitted to measurements using non-linear least-squares method resulting in $\rho_0 = 0.473$ at $\theta_i = 0$ degrees (a) and $\rho_0 = 0.457$ at $\theta_i = 20$ degrees (b).

The predictive power of the method is shown in Figs. 5 and 6 below. A value of $\rho = 0.47$ together with $\sigma_N^0 = 0.4528$, $n = 1.526$ and $k = 0.193$ has been used in the predictions.

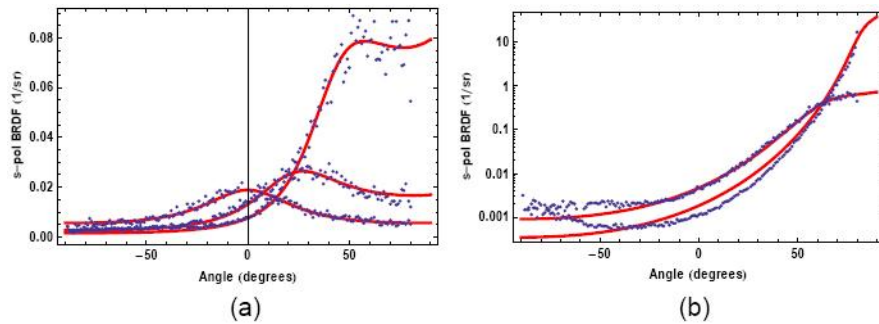


Fig. 5. Scattering from a painted surface illuminated by s-polarized radiation at $3.39 \mu\text{m}$ together with predictions based on the four parameter solution. The predictions are shown for $\theta_i = 0, 20$ and 40 degrees (a) and $\theta_i = 60$ and 80 degrees (b).

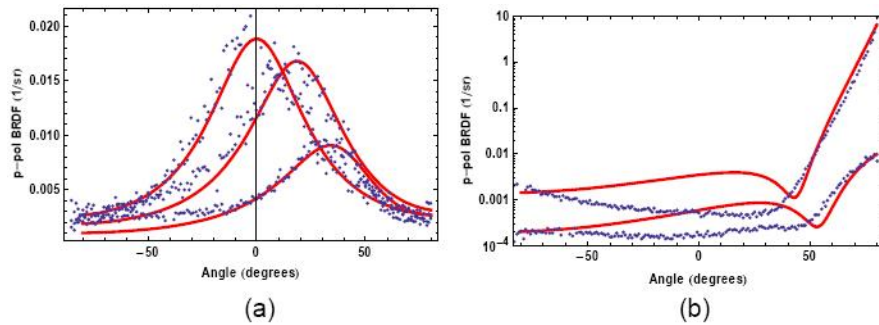


Fig. 6. Scattering from a painted surface illuminated by p-polarized radiation at $3.39 \mu\text{m}$ together with predictions based on the four parameter solution. The predictions are shown for $\theta_i = 0, 20$ and 40 degrees (a) and $\theta_i = 60$ and 80 degrees (b).

Observe that the very different appearance of p-polarized scattered radiation compared to the s-polarized scattered radiation is correctly predicted. For large angles of incidence, the prediction is still acceptable over two orders of magnitude.

4. Discussion and conclusions

We have presented a four-parameter model for BRDF that accurately matches measured polarimetric BRDF data for a painted rough surface over three orders of magnitude. The data required for fitting the model parameters are DHR measurements at both polarizations, and a

BRDF at specified angle of incidence. The aim of the procedure is to simplify the measurement process as much as possible.

Future work in this area is suggested in terms of treating depolarization effects and in further validation of the model over a range of rough surfaces. It would also be worthwhile from a practical point of view to study whether the BRDF measurement could be replaced by a diffuse directional reflectance (DDR) measurement. That would simplify the instrumentation and allow more complete in field measurements.

The normalization of the pBRDF is now performed numerically. It is of interest to find analytical solutions that fulfill the reciprocity requirement. It might be possible to find at least approximate solutions since the function seems to be numerically quite well behaved.

More complex surfaces will need extensions of the pBRDF. Enhanced backscatter is not treated within the present model. Multiple scattering processes such as e.g. combinations of surface and bulk scattering will need modifications to the present model. Those modifications can be based on physical reasoning and result in similarly well behaved modeling.

Finally, this is believed to be a novel and highly efficient approach to model the optical scattering in a painted surface.